



## ORIGINAL ARTICLE

# Preparation of highly dispersed W/Al<sub>2</sub>O<sub>3</sub> hydrodesulfurization catalysts via a microwave hydrothermal method: Effect of oxalic acid



Hao Wang<sup>\*</sup>, Zhenwei Liu, Yan Wu, Zhenyu Yao, Wanying Zhao, Weizhuo Duan, Ke Guo

School of Chemistry and Chemical Engineering, Southwest Petroleum University, Chengdu 610500, Sichuan Province, People's Republic of China

Received 19 January 2014; accepted 3 November 2014  
Available online 10 November 2014

## KEYWORDS

Hydrodesulfurization catalyst;  
Microwave hydrothermal;  
Oxalic acid;  
Dispersion;  
Metal-support interaction

**Abstract** A novel microwave hydrothermal method was developed to prepare highly dispersed W/Al<sub>2</sub>O<sub>3</sub> catalysts, in which WO<sub>3</sub> was deposited on alumina via precipitation between tungstate and nitric acid under microwave hydrothermal environment and oxalic acid was used as an additive. Moreover, the role of oxalic acid was investigated by varying its amount and the addition method. It is found that the catalysts show higher WO<sub>3</sub> dispersion and weaker W–Al interaction than that prepared by the conventional impregnation method. The hydrothermal period can be extremely reduced to a few minutes, and highly dispersed WO<sub>3</sub> can be achieved even without oxalic acid. When oxalic acid was added after the formation of H<sub>2</sub>WO<sub>4</sub>, it mainly acts as a modifier for reacting with the hydroxyl groups on alumina and has little effect on WO<sub>3</sub> dispersion. When oxalic acid was divided into two parts, one for pretreating alumina and the remains for preventing the aggregation of H<sub>2</sub>WO<sub>4</sub>, it may effectively act as both dispersant and modifier, leading to further increased WO<sub>3</sub> dispersion and weakened W–Al interaction. The catalysts prepared by the microwave hydrothermal method show superior dibenzothiophene hydrodesulfurization activity. This method provides rapidity, convenience and cost effectiveness for preparing active hydrotreating catalysts.

© 2014 The Authors. Production and hosting by Elsevier B.V. on behalf of King Saud University. This is an open access article under the CC BY-NC-ND license (<http://creativecommons.org/licenses/by-nc-nd/3.0/>).

<sup>\*</sup> Corresponding author at: School of Chemistry and Chemical Engineering, South West Petroleum University, Xindu Avenue 8<sup>#</sup>, Xindu District, Chengdu City 610500, Sichuan Province, People's Republic of China. Tel.: +86 28 83037338; fax: +86 28 83037305.

E-mail address: [wanghaoswpu@hotmail.com](mailto:wanghaoswpu@hotmail.com) (H. Wang).

Peer review under responsibility of King Saud University.



Production and hosting by Elsevier

## 1. Introduction

In recent years, the demand of clean diesel with low sulfur content is growing rapidly because of more stringent environmental regulations. Hydrodesulfurization (HDS) is the main industrial process to reduce sulfides in fuel (Klimova et al., 2013). Compared with upgrading hydrotreating equipment or increasing the severity of HDS conditions, the development of highly active hydrotreating catalysts is a more effective

and economical way to achieve deep HDS (Babich and Moulijn, 2003).

Alumina-supported sulfided Ni(Co)–W(Mo) catalysts are extensively used for hydrotreating of diesel. Intensive efforts are underway to enhance the activity of the catalysts. Many researchers have focused on new mesoporous supports with ordered pore structure, larger pore size and higher surface area than the conventional alumina, such as MCM-41 (Hussain et al., 2013), SBA-15 (Li et al., 2012), SBA-16 (Huirache et al., 2012), and HMS (Zepeda et al., 2014). Another approach receiving considerable attention is the introduction of chelating agents, such as citric acid (Rinaldi et al., 2010), nitriloacetic acid (Lélias et al., 2009), 1,2-cyclohexanediamine-tetraacetic acid (Koizumi et al., 2010) and ethylenediaminetetraacetic acid (Rana et al., 2007). These chelating agents can form stable complexes with Ni or Co promoters to retard their sulfidation and produce more Ni(Co)–W(Mo)-S type II active phases. Moreover, the combination of mesoporous support and chelating agents has also attracted increasing attention in the latest years (Badoga et al., 2012; Klimova et al., 2013; Peña et al., 2014; Wu et al., 2014). However, most of the studies are based on the conventional impregnation method; less attention has been paid on developing novel catalyst preparation methods to improve the performance of alumina-supported hydrotreating catalysts without adding expensive chelating agents.

It is accepted that an effective way to prepare highly active HDS catalysts is improving the dispersion of active metal and weakening the metal–alumina interaction (Olivas and Zepeda, 2009; Vissenberg et al., 2001). Nevertheless, due to the aggregation of active species, the conventional impregnation method generally leads to poor metal dispersion, and hence the limited loading of active metal (Liu et al., 2007). Moreover, the strong metal–alumina interaction readily forms due to the reaction between the aluminum hydroxyl groups and metal precursors (Sun et al., 2003). Recently, an oxalic acid (Wang et al., 2008) or hexadecyltrimethyl ammonium bromide (CTAB) (Fan et al., 2007; Wang et al., 2007) assisted hydrothermal deposition method (HD) was introduced to prepare W/Al<sub>2</sub>O<sub>3</sub> and NiW/Al<sub>2</sub>O<sub>3</sub> hydrotreating catalysts with both highly dispersed WO<sub>3</sub> and weak tungsten–alumina interaction, in which oxalic acid or CTAB can prevent the aggregation of WO<sub>3</sub> and modify the surface of alumina, and the hydrothermal environment may promote the distribution of WO<sub>3</sub> on alumina. The HD method increases the HDS and HDN activity significantly, but it suffers from the long hydrothermal

treatment period (12 h), especially at high tungsten loadings, inevitably leading to serious breakage of catalyst and large energy expenditure.

Microwave hydrothermal method is a genuine low temperature and high reacting rate method due to direct interaction of radiation with molecular (Moreira et al., 2008). During the past decade, the microwave hydrothermal method has been successfully used to synthesize various nano-sized materials (Huang et al., 2010; Su et al., 2010; Zhu and Hang, 2013). This method is superior to the conventional hydrothermal method in fast and uniform heating as well as rapid kinetics of crystallization (Komarneni et al., 1999). However, to our knowledge, the microwave hydrothermal method is seldom used to deposit active metal oxide on pre-synthesized support for preparing hydrotreating catalysts. In the present work, a microwave hydrothermal method (MWH) was developed to prepare W/Al<sub>2</sub>O<sub>3</sub> hydrotreating catalyst with both high WO<sub>3</sub> dispersion and weak tungsten–alumina interaction, which requires significantly less time and energy than the previous HD method. In addition, the role of oxalic acid was also investigated through varying its amount and the addition method.

## 2. Experimental

### 2.1. Catalyst preparation

A series of W/Al<sub>2</sub>O<sub>3</sub> catalysts with the same WO<sub>3</sub> loading were prepared by MWH. Firstly, 1.5 g  $\gamma$ -alumina (Sasol GmbH, Germany, 20–40 mesh) and 19.3 ml of 0.1 M ammonium metatungstate (AMT) solution were mixed in a microwave digestion vessel (volume of 80 ml and diameter of 35 mm), and then diluted HNO<sub>3</sub> was added to produce H<sub>2</sub>WO<sub>4</sub> precipitation. Secondly, various amounts of 0.8 M oxalic acid solution were added into the suspension under stirring. Thirdly, the digestion vessel was sealed and irradiated in a microwave oven at 600 W (2.45 GHz) for 5 min. Finally, the product was cooled, filtered and dried at 110 °C for 2 h followed by calcination at 550 °C for 4 h. The corresponding catalysts were named as MWH-X, where X represents the molar ratio of oxalic acid to W. The WO<sub>3</sub> contents of the catalysts determined by X-ray fluorescence spectroscopy (XRF) (AXIOS, PANalytical, The Netherlands) are listed in Table 1.

To further investigate the role of oxalic acid, the same amount of oxalic acid with a mole ratio of oxalic acid to W = 0.5 was introduced by three methods. For method A, all oxalic acid was used to pretreat alumina through impregnating alumina

**Table 1** WO<sub>3</sub> content, specific surface area, pore volume and surface W/Al ratio of the W/Al<sub>2</sub>O<sub>3</sub> catalysts.

Sample	WO <sub>3</sub> content (wt%)	Specific surface area (m <sup>2</sup> g <sup>-1</sup> )	Pore volume (cm <sup>3</sup> g <sup>-1</sup> )	Surface atom ratio of W/Al
Al <sub>2</sub> O <sub>3</sub>	–	214.6	0.54	–
IM	23.1	153.5	0.35	0.052
MWH-0	22.9	171.9	0.43	0.071
MWH-0.25	23.1	176.7	0.44	0.070
MWH-0.5*	23.0	178.6	0.44	0.073
MWH-A	22.9	165.1	0.40	0.063
MWH-B	22.8	189.4	0.47	0.087

\* MWH-0.5 is identical to MWH-C.

under microwave irradiation for 2 min. For method B, half of oxalic acid was used to pretreat alumina and half of oxalic acid was added after the formation of  $\text{H}_2\text{WO}_4$  as described above. For method C, all oxalic acid was added after the formation of  $\text{H}_2\text{WO}_4$ . The resulting catalysts were named as MWH-A, MWH-B and MWH-C, respectively. Their  $\text{WO}_3$  contents were also measured by XRF and are listed in Table 1.

The  $\text{WO}_3$  content of the catalysts prepared by MWH are controlled at nearly 23 wt%. Therefore, for comparison, a  $\text{W}/\text{Al}_2\text{O}_3$  catalyst with the same  $\text{WO}_3$  content (Table 1) referred as catalyst IM was prepared by a conventional impregnation method. The alumina support was impregnated with AMT solution at room temperature for 12 h, and then dried at 110 °C for 2 h and calcined at 550 °C for 4 h.

## 2.2. Catalyst characterization

X-ray diffraction (XRD) patterns were recorded on an X'Pert Pro diffractometer (Panalytical, Netherlands) equipped with an X'Celerator detector, using  $\text{Cu K}\alpha$  radiation and operating at 40 kV and 40 mA. The scanning was made from 10° to 80° ( $2\theta$ ) with a step size of 0.02° and a step time of 12 s.

X-ray photoelectron spectroscopy (XPS) measurement was carried out on a Thermo Fisher K-Alpha spectrometer (Thermo Fisher, USA) using  $\text{K}\alpha$  Al radiation. Peak shifts due to charging of the samples were corrected by taking the  $\text{Al}2p$  line of  $\text{Al}_2\text{O}_3$  at 74.0 eV as a reference (Zuo et al., 2004).

The surface area and pore volume of the catalysts were measured with a Quadrasorb SI analyzer (Quantachrome, USA) at -195 °C using liquid  $\text{N}_2$ . All samples were degassed at 300 °C for 6 h in vacuum before analysis.

The temperature programmed reduction (TPR) analyses of the catalysts were performed on an AutoChem II 2920 chemisorption analyzer (Micromeritics, USA) equipped with a thermal conductivity detector (TCD). The sample was pretreated in an Ar flow at 300 °C for 1 h and then cooled down to room temperature. Subsequently, the sample was heated to 1000 °C at a rate of 10 °C/min in a 10 v%  $\text{H}_2/\text{Ar}$  flow.

Fourier transform infrared (FT-IR) spectra of the catalysts were recorded on a WQ 520 spectrophotometer (Beifen, China) using the KBr pellet technique at room temperature. A total of 32 scans were taken with a resolution of 2  $\text{cm}^{-1}$ .

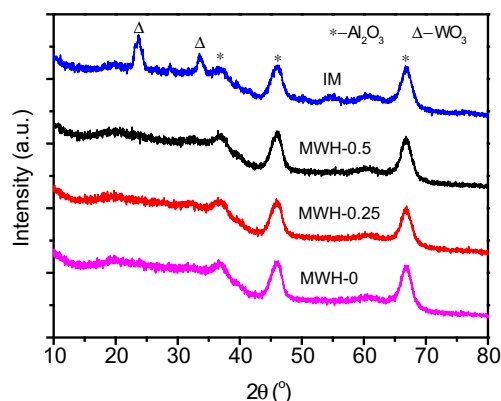


**Figure 1** XRD patterns of the  $\text{W}/\text{Al}_2\text{O}_3$  catalysts with different oxalic acid amounts.

## 2.3. Catalyst test

HDS experiments were performed on a KLJH-4010 fixed-bed microreactor (KLC, China). Prior to reaction, 1 ml catalyst (0.92 g) was sulfided using 3 wt%  $\text{CS}_2$  in cyclohexane at 300 °C, total pressure of 4.0 MPa, liquid volume hourly space velocity (LHSV) of 10.0  $\text{h}^{-1}$  and  $\text{H}_2$ /hydrocarbon volumetric ratio of 400 for 4 h. Then, the feed was switched to 1 wt% DBT in cyclohexane and the HDS reaction was carried out under 300 °C, 4 MPa, LHSV 10  $\text{h}^{-1}$  and  $\text{H}_2$ /hydrocarbon 400. After reaching a steady state, the liquid product was collected and analyzed by a 9790II gas chromatography (Fuli, China) equipped with FID detector and KB-5 capillary column (30 m  $\times$  0.32 mm  $\times$  0.25  $\mu\text{m}$ , Kromat, USA). The rate constant of DBT HDS and turnover frequency (TOF) of catalysts were calculated according to the reference (Wang et al., 2008).

## 3. Results and discussion

### 3.1. Effect of oxalic acid amount

The XRD patterns of catalysts IM, MWH-0, MWH-0.25 and MWH-0.5 are presented in Fig. 1. The peaks at 23.6° and 33.6° attributed to orthorhombic  $\text{WO}_3$  (ICDD PDF 00-020-1324) are observed on the XRD pattern of catalyst IM, whereas only peaks at 45.8° and 66.7° ascribed to cubic  $\gamma$ -alumina (ICDD PDF 01-075-0921) are present on the XRD patterns of MWH-0, MWH-0.25 and MWH-0.5. This indicates that  $\text{WO}_3$  species are highly dispersed on the catalysts prepared by MWH while poorly dispersed on the catalyst prepared by IM.

To further study the dispersion of  $\text{WO}_3$ , the four catalysts were characterized by XPS. Their surface atom ratios of tungsten to aluminum are listed in Table 1. As expected, the  $\text{W}/\text{Al}$  ratios of catalysts MWH are higher than that of catalyst IM. Nevertheless, it seems that the amount of oxalic acid gives little effect on the  $\text{WO}_3$  dispersion of catalysts MWH, since the differences in their  $\text{W}/\text{Al}$  ratios are less than 5%. The XRD and XPS results demonstrate that the high  $\text{WO}_3$  dispersion of catalysts MWH can be predominantly attributed to the microwave hydrothermal environment instead of oxalic acid. As reported previously (Wang et al., 2008), the increased  $\text{WO}_3$  dispersion in conventional HD method is attributed to both high mass transfer ability of hydrothermal solution and anti-aggregation effect of oxalic acid that can act as a dispersant by adsorbing on tungstic acid colloids via H-bonding between the carboxyl group of oxalic acid and negative charged tungstic acid. If the oxalic acid or other dispersant is absent, the HD method can hardly disperse  $\text{WO}_3$  uniformly and the bulk  $\text{WO}_3$  are present on alumina. However, the microwave hydrothermal environment can highly disperse  $\text{WO}_3$  on alumina without the assistance of oxalic acid, which is related to at least two reasons. First, microwave hydrothermal treatment allows for rapid heating and localized high temperature, and thus accelerates the nucleation and recrystallization of tungstic acid and extremely inhibits the crystallite growth, resulting in small nano-sized species (Komarneni et al., 1999; Glaspell et al., 2005). Second, the mobility of tungsten species under the hydrothermal condition can be further promoted by the increase in the effective collision rate of tungstic acid that acts

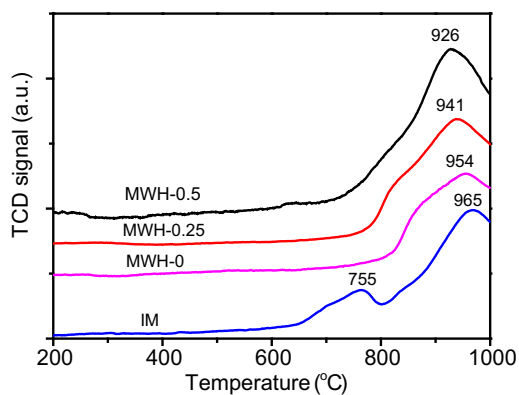


**Figure 2** TPR profiles of the W/Al<sub>2</sub>O<sub>3</sub> catalysts with different oxalic acid amounts.

as a strong microwave absorber at 2.45 GHz (Sun et al., 2008), which is helpful to disperse tungsten on alumina homogeneously and quickly. On the contrary, the conventional heating in hydrothermal process relies on thermal conduction and results in the long heating period, inhomogeneous temperature profiles within the autoclave and slow reaction and crystallization kinetics, leading to slow nucleation and excess growth of the products (Zhu and Hang, 2013), as well as the less enhanced mobility of tungsten species. As a result, a large amount of oxalic acid is required to prevent H<sub>2</sub>WO<sub>4</sub> from aggregation for the HD method.

The surface area and pore volume of the four catalysts are also listed in Table 1. Among them, catalyst IM shows the lowest surface area and pore volume, due to the serious pore blockage by agglomerated WO<sub>3</sub> crystallites (Calderón et al., 2014). MWH-0.5 shows a little higher surface area than MWH-0, because the formation of oxalate bridges between oxalic acid and alumina may suppress the reduction of alumina surface area caused by hydrothermal treatment (Absi-Halabi et al., 1993).

The TPR profiles of the W/Al<sub>2</sub>O<sub>3</sub> catalysts are shown in Fig. 2. An apparent peak in 900–1000 °C present on the profiles of all catalysts is ascribed to the reduction of supported WO<sub>3</sub> (Fan et al., 2007). The peak at 755 °C is only observed on the profile of catalyst IM, owing to the reduction of bulk WO<sub>3</sub> (Reyes et al., 1994). Compared to catalyst IM, the reduction peaks of catalysts MWH shift to lower temperatures. It is known that the reaction between the carboxyl groups of oxalic acid and the hydroxyl groups of alumina can weaken the tungsten–alumina interaction (Wang et al., 2008). Therefore, the reduction peak temperature decreases with the increasing amount of oxalic acid. However, when oxalic acid is absent, MWH-0 also shows weaker tungsten–alumina interaction than catalyst IM, which may be attributed to the lower pH of precursor solution in the former, because the higher impregnation pH may slightly increase the relative amount of less reducible dispersed isolated WO<sub>x</sub> species (Cruz et al., 2002).

The above characterization results clearly reveal that the MWH method can increase the dispersion of WO<sub>3</sub> and weaken the tungsten–alumina interaction in comparison with the conventional IM method. Moreover, this method differs from the previous HD method in the role of oxalic acid: in the former, oxalic acid mainly acts as a modifier to weaken the strong tungsten–alumina interaction, whereas in the latter, besides modifying alumina support, oxalic acid also acts as a dispersant to prevent

the aggregation of WO<sub>3</sub> and increase the dispersion. As a result, to attain the similar promotion effect on WO<sub>3</sub> dispersion and tungsten–alumina interaction, HD may require more oxalic acid than MWH, which can be confirmed by the fact that if the mole ratio of oxalic acid to W is less than 1, bulk WO<sub>3</sub> crystallites are formed on W/Al<sub>2</sub>O<sub>3</sub> at the WO<sub>3</sub> content of 23 wt%.

The HDS activity of the W/Al<sub>2</sub>O<sub>3</sub> is listed in Table 2. Catalysts MWH show higher activity and TOF than catalyst IM, due to the higher WO<sub>3</sub> dispersion and weaker tungsten–alumina interaction, which often lead to the more exposed or shorter metal sulfide active phase and the higher sulfidation degree (Wang et al., 2007). Moreover, the larger WO<sub>3</sub> crystallites on catalyst IM promote the blocking of even filling of pores, making difficult diffusion of reactants (Montesinos-Castellanos et al., 2007). Even without oxalic acid, the rate constant and TOF of MWH-0 are increased by 36.7% and 32.5%, respectively, as compared with catalyst IM. For catalysts MWH, although the dispersion of WO<sub>3</sub> was nearly unchanged, the increased oxalic acid further weakens the tungsten–alumina interaction, which facilitates the sulfidation of WO<sub>3</sub> and thus enhances the HDS activity.

### 3.2. Effect of oxalic acid addition method

As discussed above, when oxalic acid was added after the formation of H<sub>2</sub>WO<sub>4</sub>, the increase in oxalic acid amount has a small promotion effect on WO<sub>3</sub> dispersion. Therefore, three different oxalic acid addition methods were attempted to further modify the dispersion and tungsten–alumina interaction of W/Al<sub>2</sub>O<sub>3</sub> at the same oxalic acid amount (mole ratio of oxalic acid to W = 0.5).

The XRD patterns of MWH-A, MWH-B and MWH-C are given in Fig. 3. In all patterns, only diffraction peaks ascribed to alumina are observed, indicating highly dispersed WO<sub>3</sub>.

The surface atom ratios of tungsten to aluminum determined by XPS are also listed in Table 1. It is interesting to find that MWH-B shows 19.2% higher W/Al ratio than MWH-C, while MWH-A shows 13.7% lower W/Al ratio than MWH-C.

The surface area and pore volume of MWH-A, MWH-B and MWH-C are listed in Table 1. The surface area and pore volume follow the order of MWH-B > MWH-C > MWH-A, due to the variation of WO<sub>3</sub> dispersion.

The TPR profiles of MWH-A, MWH-B and MWH-C are shown in Fig. 4. It is clear that the temperature of reduction peak is in the order of MWH-C > MWH-B > MWH-A.

**Table 2** The DBT HDS activity of catalysts.

Sample	Rate constant (10 <sup>-4</sup> × mol g <sup>-1</sup> h <sup>-1</sup> )	TOF (10 <sup>-1</sup> × h <sup>-1</sup> )
IM	0.98	0.89
MWH-0	1.34	1.18
MWH-0.25	1.40	1.22
MWH-0.5 <sup>*</sup>	1.48	1.28
MWH-A	1.55	1.32
MWH-B	1.81	1.51
NiW-MWH-B	3.19	2.32
Commercial NiW catalyst	2.35	1.81

<sup>\*</sup> MWH-0.5 is identical to MWH-C.

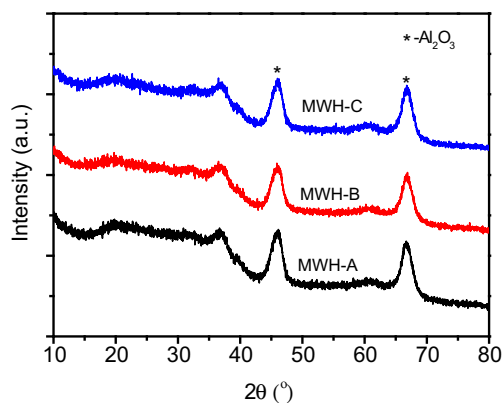


**Figure 3** XRD patterns of the W/Al<sub>2</sub>O<sub>3</sub> catalysts with different oxalic acid addition methods.

Despite the identical oxalic acid amount, the different addition methods of oxalic acid impose different modification effects on both WO<sub>3</sub> dispersion and tungsten–alumina interaction. During the catalyst preparation process, oxalic acid could exert two roles: reacting with the aluminum hydroxyl groups and adsorbing on tungstic acid. For method A, all oxalic acid was used to pretreat alumina and hence greatly reduce the amount of aluminum hydroxyl groups, causing the remarkable decreased tungsten–alumina interaction, however, this also results in no excess oxalic acid adsorbing on H<sub>2</sub>WO<sub>4</sub> colloids to prevent their aggregation. Moreover, at high oxalic acid loading, the corrosion of acid on alumina is increased, leading to the decrease in surface area (Atanasova et al., 1997) (Table 1). Therefore, MWH-A has the lowest tungsten dispersion and weakest tungsten–alumina interaction among the three catalysts. For method B, the oxalic acid could be departed into two parts, one for pretreating alumina to react with the hydroxyl groups on alumina, the other for interacting with H<sub>2</sub>WO<sub>4</sub> colloids. As an acidic molecular, oxalic acid will preferentially react with the basic hydroxyl groups on alumina (Sun et al., 2003). Herein, the total amount of hydroxyl groups on alumina is 1.71 mmol g<sup>-1</sup>(Al<sub>2</sub>O<sub>3</sub>) determined by thermogravimetry according to Jiang's (1994) method. The oxalic acid for pretreating alumina is 0.32 mmol g<sup>-1</sup>(Al<sub>2</sub>O<sub>3</sub>), accounting for 18.7% of the total amount of hydroxyl groups on alumina, which is close to the percentage of basic hydroxyl groups (15%) on alumina reported by Sun et al. (2003). It indicates that the oxalic acid used for pretreatment may selectively react

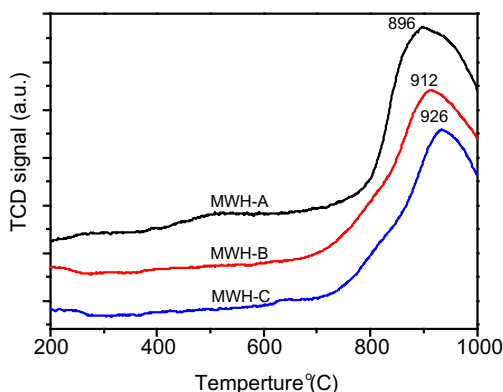


**Figure 4** TPR profiles of the W/Al<sub>2</sub>O<sub>3</sub> catalysts with different oxalic acid addition methods.

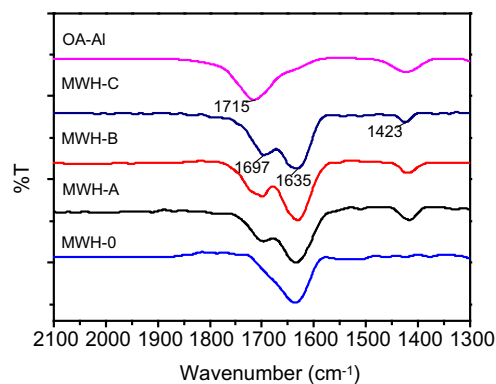


**Figure 5** FT-IR spectra of the W/Al<sub>2</sub>O<sub>3</sub> catalysts before calcination.

with the basic hydroxyl groups that most readily react with tungsten species to form strong tungsten–alumina interaction. Furthermore, the pretreated alumina surface could reduce the adsorption of the oxalic acid added after the formation of H<sub>2</sub>WO<sub>4</sub>, allowing oxalic acid to prevent the aggregation of H<sub>2</sub>WO<sub>4</sub> more effectively (Li et al., 2011). For method C, all oxalic acid was introduced after the formation of H<sub>2</sub>WO<sub>4</sub>. On the one hand, tungsten species and oxalic acid will adsorb competitively on the surface of alumina, which inevitably leads to the formation of strong interaction between tungsten and alumina (Li et al., 2011), therefore, MWH-C shows stronger tungsten–alumina interaction than MWH-B and MWH-A. On the other hand, oxalic acid will adsorb on alumina and H<sub>2</sub>WO<sub>4</sub> randomly, which may cause a relatively small amount of oxalic acid to form hydrogen bonding with H<sub>2</sub>WO<sub>4</sub>, therefore, the WO<sub>3</sub> dispersion of MWH-C lies between MWH-B and MWH-A.

The FT-IR spectra of the W/Al<sub>2</sub>O<sub>3</sub> catalysts prepared by MWH before calcination are shown in Fig. 5. For MWH-0, the only evident peak at 1635 cm<sup>-1</sup> corresponding to vibration of O–H is observed (Abadleh and Grassian, 2002). For MWH-A, MWH-B and MWH-C, the peak at 1697 cm<sup>-1</sup> ascribed to stretching vibration of C=O of carboxylic acid and the peak at 1423 cm<sup>-1</sup> ascribed to symmetric vibrations of carboxylate ions are present (Wang et al., 2008), indicating that oxalic acid can form carboxylate with the hydroxyl groups on alumina surface. This proves that the reaction between oxalic acid and hydroxyl groups on alumina can be achieved within the short time of microwave hydrothermal treatment. To verify the interaction of oxalic acid with H<sub>2</sub>WO<sub>4</sub>, pure alumina impregnated with oxalic acid (named as OA-Al) was also prepared and characterized by FT-IR, and the pattern is given in Fig. 5. It is noted that, the peak ascribed to oxalic acid at 1715 cm<sup>-1</sup> in the spectrum of OA-Al, shifts to lower wavenumber in catalysts MWH, suggesting the formation of H-bond between oxalic acid and H<sub>2</sub>WO<sub>4</sub>. For MWH-B, the peak assigned to carboxylic acid is stronger than MWH-C and MWH-A, which suggests more oxalic acid can interact with H<sub>2</sub>WO<sub>4</sub> to provide anti-aggregation effect. Moreover, the peak intensity of carboxylate in MWH-A is much higher than that of MWH-B and MWH-C, suggesting the formation of more carboxylate, which leads to the weaker tungsten–alumina interaction.

The HDS activity is listed in Table 2. MWH-B shows much higher activity than MWH-A and MWH-C, which can be

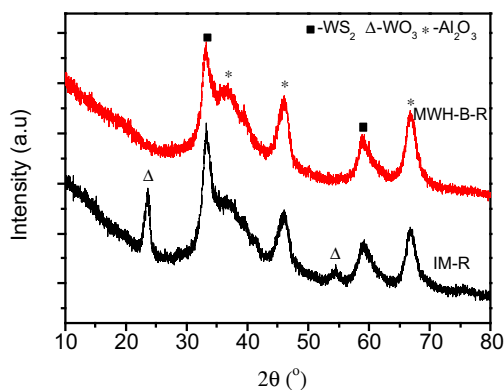


**Figure 6** XRD patterns of catalysts MWH-B-R and IM-R.

attributed to both the further increased WO<sub>3</sub> dispersion and weakened tungsten–alumina interaction. It is worthy to note that MWH-A shows a little higher activity than MWH-C, although the latter has better WO<sub>3</sub> dispersion, since the weak tungsten–alumina interaction can not only increase the sulfidation degree of WO<sub>3</sub> but also may increase the stacking degree of tungsten sulfides, which is favorable in planar adsorption of DBT on the active sites (Hensen et al., 2001).

From Table 2, it reveals that when the MWH method is used and only oxalic acid amount is increased to 0.5 (mole ratio of oxalic acid to W), the HDS rate constant and TOF are 51.0% and 43.8% higher than those of catalyst IM, however, when the oxalic acid addition method B is used, the data are increased by 84.7% and 69.7%, respectively. This is due to the fact that method B can offer much more positive modification effects.

After HDS reaction, catalysts MWH-B and IM were collected and named as MWH-B-R and IM-R, respectively. Their XRD patterns are shown in Fig. 6. Besides the diffraction peaks of alumina support, the peaks at about 33.2° and 59.1° ascribed to hexagonal WS<sub>2</sub> phase (ICDD PDF 00-008-0237) appear on both catalysts, indicating the sulfidation of WO<sub>3</sub>. However, the peaks at 23.6° and 54.5° ascribed to orthorhombic WO<sub>3</sub> (ICDD PDF 00-020-1324) are only present on IM-R, similar to its oxidic precursor, suggesting the incomplete sulfidation of WO<sub>3</sub>. The presence of (110) reflection at 2θ = 59.1° is representative of WS<sub>2</sub> slab layer (Yi et al., 2011), therefore, the slab size can be calculated by the Scherrer relation. The size is 4.2 nm for MWH-B-R and 5.6 nm for IM-R, respectively, indicating better WS<sub>2</sub> dispersion on the former, in line with the XRD and XPS results of their oxidic precursors. The XRD result of catalysts after reaction confirms that the HDS activity enhancement over MWH-B could be attributed to both higher dispersion of WS<sub>2</sub> and sulfidation degree of WO<sub>3</sub>.

The industrial HDS catalysts are composed of W and Ni, therefore, a NiW/Al<sub>2</sub>O<sub>3</sub> catalyst named as NiW-MWH-B was prepared, wherein WO<sub>3</sub> was deposited on alumina by the MWH method (like MWH-B) and then NiO was introduced by impregnating nickel nitrate on W/Al<sub>2</sub>O<sub>3</sub>. The NiO and WO<sub>3</sub> contents were controlled at 2.7 wt% and 23 wt%, respectively, close to a reference commercial NiW/Al<sub>2</sub>O<sub>3</sub> hydrotreating catalyst containing 2.9 wt% NiO and 23.6 wt% WO<sub>3</sub>. The HDS activity for DBT over the two NiW catalysts is listed in Table 2. It is clear that NiW-MWH-B shows the much higher activity and efficiency of

active sites than the commercial one. Moreover, the stability of NiW-MWH-B was tested by prolonging the HDS reaction time to 100 h, and no obvious deactivation is observed.

#### 4. Conclusions

A novel MWH method was developed to prepare highly dispersed W/Al<sub>2</sub>O<sub>3</sub> catalysts and the effect of oxalic acid amount and the addition method on property of catalyst was investigated. Compared to the conventional IM method, the MWH method can increase the dispersion of WO<sub>3</sub> and weaken the tungsten–alumina interaction. Compared to the previously reported HD method, the catalyst preparation period can be reduced dramatically from 12 h to 5 min, moreover, the highly dispersed WO<sub>3</sub> can be achieved in the absence of oxalic acid. This is attributed to the rapid nucleation and greatly inhibited growth of tungstic acid colloids as well as the enhanced mobility of tungsten species, induced by the microwave hydrothermal environment.

When oxalic acid is added after the formation of tungstic acid, due to its complete adsorption on both alumina and tungstic acid, it mainly plays a role in reacting with the hydroxyl groups on alumina to weaken the tungsten–alumina interaction, therefore, the increased amount of oxalic acid has a slight effect on WO<sub>3</sub> dispersion. At the same oxalic acid amount, the addition method of oxalic acid has a significant influence on the catalyst. By using a part of oxalic acid to pre-treat alumina and the remaining to adsorb on tungstic acid colloids, oxalic acid can effectively act as both a modifier to interact with alumina and a dispersant to prevent tungstic acid colloids from aggregation. As a result, the corresponding catalyst shows further increased WO<sub>3</sub> dispersion and weakened tungsten–alumina interaction. The catalyst prepared by the MWH method has superior HDS activity than the catalyst prepared by the IM method. It is hoped that this method may provide a rapid and efficient way to prepare highly active hydrotreating catalysts with low energy costs.

#### Acknowledgments

The authors acknowledge the financial support from the National Natural Science Foundation of China (20906075) and Foundation of State Key Laboratory of Oil and Gas Reservoir Geology and Exploitation (PLN1127).

#### References

- Abadleh, H.A., Grassian, V.H., 2002. FT-IR study of water adsorption on aluminum oxide surfaces. *Langmuir* 19, 341–347.
- Abasi-Halabi, M., Stanislaus, A., Al-Zaid, H., 1993. Effect of acidic and basic vapors on pore size distribution of alumina under hydrothermal conditions. *Appl. Catal. A* 101, 117–128.
- Atanasova, P., Tabakova, T., Vladov, C., Halachev, T., Agudo, A.L., 1997. Effect of phosphorus concentration and method of preparation on the structure of the oxide form of phosphorus–nickel–tungsten/alumina hydrotreating catalysts. *Appl. Catal. A* 161, 105–119.
- Babich, I.V., Moulijn, J.A., 2003. Science and technology of novel processes for deep desulfurization of oil refinery streams: a review. *Fuel* 82, 607–631.
- Badoga, S., Mouli, K.C., Soni, K.K., Dalai, A.K., Adjaye, J., 2012. Beneficial influence of EDTA on the structure and catalytic

- properties of sulfided NiMo/SBA-15 catalysts for hydrotreating of light gas oil. *Appl. Catal. B* 125, 67–84.
- Calderón, M.Á., Nieto, J.A., Klimova, T.E., 2014. Effect of the amount of citric acid used in the preparation of NiMo/SBA-15 catalysts on their performance in HDS of dibenzothiophene-type compounds. *Catal. Today* 220–222, 78–88.
- Cruz, J., Avalos, B.M., López, C.R., Bañares, M.A., Fierro, J.L.G., Palacios, J.M., López, A., 2002. Influence of pH of the impregnation solution on the phosphorus promotion in W/Al<sub>2</sub>O<sub>3</sub> hydro-treating catalysts. *Appl. Catal. A* 224, 97–110.
- Fan, Y., Bao, X.J., Wang, H., Chen, C.F., Shi, G., 2007. A surfactant-assisted hydrothermal deposition method for preparing highly dispersed W/ $\gamma$ -Al<sub>2</sub>O<sub>3</sub> hydrodenitrogenation catalyst. *J. Catal.* 245, 477–481.
- Glaspell, G., Fuoco, L., El-Shall, M.S., 2005. Microwave synthesis of supported Au and Pd nanoparticle catalysts for CO oxidation. *J. Phys. Chem. B* 109, 17350–17355.
- Hensen, E.J.M., Kooyman, P.J., Meer, Y., Kraan, A.M., Beer, V.H.J., Veen, J.A.R., Santen, R.A., 2001. The relation between morphology and hydrotreating activity for supported MoS<sub>2</sub> particles. *J. Catal.* 199, 224–235.
- Huang, H., Sithambaram, S., Chen, C.H., Kithongo, C.K., Xu, L., Iyer, A., Garces, H.F., Suib, S.L., 2010. Microwave-assisted hydrothermal synthesis of cryptomelane-type octahedral molecular sieves (OMS-2) and their catalytic studies. *Chem. Mater.* 22, 3664–3669.
- Huirache, A.R., Pawelec, B., Loricera, C.V., Rivera, E.M., Nava, R., Torres, B., Fierro, J.L.G., 2012. Comparison of the morphology and HDS activity of ternary Ni(Co)-Mo-W catalysts supported on Al-HMS and Al-SBA-16 substrates. *Appl. Catal. B* 125, 473–485.
- Hussain, M., Song, S.K., Ihm, S.K., 2013. Synthesis of hydrothermally stable MCM-41 by the seed crystallization and its application as a catalyst support for hydrodesulfurization. *Fuel* 106, 787–792.
- Jiang, Z.X., Meng, S.C., Yu, Y.Q., Li, C.H., Xin, Q., 1994. The qualitative and quantitative study of the interaction between molybdate and surface hydroxyl groups on  $\gamma$ -Al<sub>2</sub>O<sub>3</sub>. *Chin. J. Catal.* 15, 387–390.
- Klimova, T.E., Valencia, D., Mendoza, J.A., Hernández, H.P., 2013. Behavior of NiMo/SBA-15 catalysts prepared with citric acid in simultaneous hydrodesulfurization of dibenzothiophene and 4,6-dimethyldibenzothiophene. *J. Catal.* 304, 29, 29–4.
- Koizumi, N., Hamabe, Y., Yoshida, S., Yamada, M., 2010. Simultaneous promotion of hydrogenation and direct desulfurization routes in hydrodesulfurization of 4,6-dimethyldibenzothiophene over NiW catalyst by use of SiO<sub>2</sub>-Al<sub>2</sub>O<sub>3</sub> support in combination with *trans*-1,2-diaminocyclohexane-*N,N,N',N'*-tetraacetic acid. *Appl. Catal. A* 383, 79–88.
- Komarneni, S., Rajha, R.K., Katsuki, H., 1999. Microwave-hydrothermal processing of titanium dioxide. *Mater. Chem. Phys.* 61, 50–54.
- Lélias, M.A., Kooyman, P.J., Mariey, L., Oliviero, L., Travert, A., Gestel, J., Veen, J.A.R., Maugé, F., 2009. Effect of NTA addition on the structure and activity of the active phase of cobalt-molybdenum sulfide hydrotreating catalysts. *J. Catal.* 267, 14–23.
- Li, H.F., Li, M.F., Chu, Y., Liu, F., Nie, H., 2011. Essential role of citric acid in preparation of efficient NiW/Al<sub>2</sub>O<sub>3</sub> HDS catalysts. *Appl. Catal. A* 403, 75–82.
- Li, Y., Pan, D.H., Yu, C.Z., Fan, Y., Bao, X.J., 2012. Synthesis and hydrodesulfurization properties of NiW catalyst supported on high-aluminum-content, highly ordered, and hydrothermally stable Al-SBA-15. *J. Catal.* 286, 124–136.
- Liu, F., Xu, S.P., Cao, L., Chi, Y., Zhang, T., Xue, D.F., 2007. A comparison of NiMo/Al<sub>2</sub>O<sub>3</sub> catalysts prepared by impregnation and coprecipitation methods for hydrodesulfurization of dibenzothiophene. *J. Phys. Chem. C* 111, 7396–7402.
- Montesinos-Castellanos, A., Lima, E., de los Reyes, H.J.A., Lara, V., 2007. Fractal dimension of MoP-Al<sub>2</sub>O<sub>3</sub> catalysts and their activity in hydrodesulfurization of dibenzothiophene. *J. Phys. Chem. C* 111, 13898–13904.
- Moreira, M.L., Mambrini, G.P., Volanti, D.P., Leite, E.R., Orlandi, M.O., Pizani, P.S., Mastelaro, V.R., Paiva-Santos, C.O., Longo, E., Varela, J.A., 2008. Hydrothermal microwave: a new route to obtain photoluminescent crystalline BaTiO<sub>3</sub> nanoparticles. *Chem. Mater.* 20, 5381–5387.
- Olivas, A., Zepeda, T.A., 2009. Impact of Al and Ti ions on the dispersion and performance of supported NiMo(W)/SBA-15 catalysts in the HDS and HYD reactions. *Catal. Today* 143, 120–125.
- Peña, L., Valencia, D., Klimova, T., 2014. CoMo/SBA-15 catalysts prepared with EDTA and citric acid and their performance in hydrodesulfurization of dibenzothiophene. *Appl. Catal. B* 147, 879–887.
- Rana, M.S., Ramírez, J., Gutiérrez, A., Ancheyta, J., Cedeño, L., Maity, S.K., 2007. Support effects in CoMo hydrodesulfurization catalysts prepared with EDTA as a chelating agent. *J. Catal.* 246, 100–108.
- Reyes, J.C., Avalos, B.M., Cordero, R.L., Agudo, A.L., 1994. Influence of phosphorus on the structure and the hydrodesulfurization and hydrodenitrogenation activity of W/Al<sub>2</sub>O<sub>3</sub> catalysts. *Appl. Catal. A* 120, 147–162.
- Rinaldi, N., Kubota, T., Okamoto, Y., 2010. Effect of citric acid addition on the hydrodesulfurization activity of MoO<sub>3</sub>/Al<sub>2</sub>O<sub>3</sub> catalysts. *Appl. Catal. A* 374, 228–236.
- Su, X.T., Xiao, F., Li, Y.N., Jian, J.K., Sun, Q.J., Wang, J.D., 2010. Synthesis of uniform WO<sub>3</sub> square nanoplates via an organic acid-assisted hydrothermal process. *Mater. Lett.* 64, 1232–1234.
- Sun, M.Y., Nicosia, D., Prins, R., 2003. The effects of fluorine, phosphate and chelating agents on hydrotreating catalysts and catalysis. *Catal. Today* 86, 173–189.
- Sun, Q.J., Luo, J.M., Xie, Z.F., Wang, J.D., Su, X.T., 2008. Synthesis of monodisperse WO<sub>3</sub>·2H<sub>2</sub>O nanospheres by microwave hydrothermal process with L(+) tartaric acid as a protective agent. *Mater. Lett.* 62, 2992–2994.
- Vissenberg, M.J., Meer, Y., Hensen, E.J.M., Beer, V.H.J., Kraan, A.M., Santen, R.A., Veen, J.A.R., 2001. The effect of support interaction on the sulfidability of Al<sub>2</sub>O<sub>3</sub>- and TiO<sub>2</sub>-supported CoW and NiW hydrodesulfurization catalysts. *J. Catal.* 198, 151–163.
- Wang, H., Fan, Y., Shi, G., Liu, Z.H., Liu, H.Y., Bao, X.J., 2007. Highly dispersed NiW/ $\gamma$ -Al<sub>2</sub>O<sub>3</sub> catalyst prepared by hydrothermal deposition method. *Catal. Today* 125, 149–154.
- Wang, H., Fan, Y., Shi, G., Liu, H.Y., Bao, X.J., 2008. Preparation of hydrotreating catalysts via an oxalic acid-assisted hydrothermal deposition method. *J. Catal.* 260, 119–127.
- Wu, H., Duan, A.J., Zhao, Z., Qi, D.H., Li, J.M., Liu, B., Jiang, G.Y., Liu, J., Wei, Y.C., Zhang, X., 2014. Preparation of NiMo/KIT-6 hydrodesulfurization catalysts with tunable sulfidation and dispersion degrees of active phase by addition of citric acid as chelating agent. *Fuel* 130, 203–210.
- Yi, Y.J., Zhang, B.S., Jin, X., Wang, L., Williamsc, C.T., Xiong, G., Su, D.S., Liang, C.H., 2011. Unsupported NiMoW sulfide catalysts for hydrodesulfurization of dibenzothiophene by thermal decomposition of thiosalts. *J. Mol. Catal. A* 351, 120–127.
- Zepeda, T.A., Infantes-Molina, A., Díaz de León, J.N., Fuentes, S., Alonso-Núñez, G., Torres-Otañez, G., Pawelec, B., 2014. Hydrodesulfurization enhancement of heavy and light S-hydrocarbons on NiMo/HMS catalysts modified with Al and P. *Appl. Catal. B* 484, 108–121.
- Zhu, X.H., Hang, Q.M., 2013. Microscopical and physical characterization of microwave and microwave-hydrothermal synthesis products. *Micron* 44, 21–44.
- Zuo, D.H., Vrinat, M., Nie, H., Maugé, F., Shi, Y., Lacroix, M., Li, D.D., 2004. The formation of the active phases in sulfided NiW/Al<sub>2</sub>O<sub>3</sub> catalysts and their evolution during post-reduction treatment. *Catal. Today* 93–95, 751–760.